ISSN 1990-3413, Astrophysical Bulletin, 2016, Vol. 71, No. 4, pp. 395–407. © Pleiades Publishing, Ltd., 2016.
Original Russian Text © V.L. Afanasiev, O.K. Silchenko, I.S. Proshina, 2016, published in Astrofizicheskii Byulleten', 2016, Vol. 71, No. 4, pp. 425–438.

Stellar Population and Evolution of Galaxies in Groups: the NGC 2300 Group

V. L. Afanasiev[1*], O. K. Silchenko[2], and I. S. Proshina[2***]**

[1] *Special Astrophysical Observatory, Russian Academy of Sciences, Nizhnii Arkhyz, 369167 Russia*
[2] *Sternberg Astronomical Institute of the Moscow State University, Moscow, 119991 Russia*

Received July 29, 2016; in final form, October 10, 2016

Abstract—Using panoramic and long-slit spectroscopy at the 6-m telescope of SAO RAS, we studied the stellar population and kinematics of five early-type disc galaxies—members of the NGC 2300 group. The evolution of galaxies appears to be absolutely out of synch: while the average age of the stars in the central regions of the galaxies located close to the center of the group ranges from 2 to 7 Gyr, the peripheral spiral galaxies have old nuclei and bulges, with the ages of 10–15 Gyr. The brightest galaxy of the NGC 2300 group, which up to now has been considered to be lenticular, of the SA0 type, turned out to be extremely hot dynamically: its bulge rotates slowly, $v/\sigma = 0.06$, and the outer parts do not rotate at all. We conclude that the kinematics of the stellar component of NGC 2300 indicates that it is not a disc galaxy, but a triaxial spheroid.

DOI: 10.1134/S1990341316040039

Keywords: *galaxies: nuclei—galaxies: bulges—galaxies: stellar content—galaxies: evolution*

1. INTRODUCTION

A major portion of galaxies in the nearby Universe are members of groups: according to the estimates [1], more than half of all galaxies, 54%, within a distance of 40 Mpc from us are in groups. Most astronomers tend to the point of view that these groups are precisely the sites where galaxies undergo "pre-processing," i.e., where their star formation stops, and they pass from the blue cloud to the red sequence. Moreover, structural adjustments are also implied—the change of the morphological type to an earlier one. The dynamical properties of the environment of galaxies in groups consist of compulsory attraction of close neighboring galaxies, as well as low, of the order of a few hundred kilometers per second, velocities of mutual passing of galaxies and typical dynamical times of crossing the entire space of a group several times less than the age of the Universe. This presents favorable conditions for slow dynamical—the so-called secular [2]—evolution of galaxies. External influences may play a dominating role in the structural and dynamical evolution of galaxies in groups; moreover, they may be both the gravitational, tidal influences of neighboring galaxies and the common dark halo of the group, and gas-dynamic influences related to the frequent presence of hot intergalactic medium in massive groups.

If several galaxies are present in a group or if the time of their "life together" in a group exceeds several billion years (as predicted by the numerical models of hierarchical evolution of the large-scale structure of the Universe), then they are subject to similar influence of a common gravitational potential of the group and a common environment—a hot intergalactic gas, if it is present in the group. It then seems probable that the reorganization of the global structure, in particular, the formation of central stellar sub-systems in galaxy group members may be synchronized, i.e., the average age of the stellar population in the centers of galaxies will be the same. Practically all mechanisms of gravitational (tidal) interaction, as well as a whole set of gas-dynamic mechanisms, such as ram pressure and static compression of galactic discs by a hot intergalactic medium, lead to a central concentration of gas in the disc, with an unavoidable burst of star formation and the formation of a secondary stellar component in the nucleus and/or bulge. The detection of synchronization of the evolution of the central regions of group galaxies would be a significant argument in favor of the dominating role of external influences.

We began investigating the stellar populations in the central regions of group galaxies over ten

*E-mail: vafan@sao.ru
**E-mail: olga@sai.msu.su
***E-mail: ii.pro@mail.ru

years ago with the Multi Pupil Fiber Spectrograph MPFS/BTA. Up to now, we were able to study 2–3 galaxies in each of the seven nearby groups. The stellar population properties of the circumnuclear discs of large galaxy group members in Leo I [3] and in the NGC 5576 [4] and NGC 3169 [5] groups turned out to be the same: the latest stars have formed there rather recently, 1–3 billion years ago, despite the early type of the galaxies. In the Leo I group, with its common for all galaxies external reservoir of neutral hydrogen in the form of a giant ring [6], the circumnuclear stellar discs are also oriented in space in a similar way. Conversely, in the Leo Triplet (NGC 3623/NGC 3627/NGC 3628), the ages of the stellar population and the gas kinematics in the centers of NGC 3623 and NGC 3627 differ significantly [7], and we conclude that the triplet galaxies have accumulated into a gravitationally bound group less than one billion year ago. In the Leo II group, in which X-ray gas was known to be present, unlike in the previously mentioned groups, the circumnuclear kinematically-distinct stellar structures of two central galaxies turned out to be old. In addition, they have somewhat different mean ages of the stellar populations—6 and 10 Gyr for NGC 3608 and NGC 3607, respectively [8]. Moreover, the peripheral, lenticular group galaxies, NGC 3599 and NGC 3626, actually demonstrate ongoing star formation within their central stellar subsystems [9]. The evolution of the central regions of early-type galaxies in the rich massive group NGC 80 [10], which also has a X-ray halo, is also asynchronous. Seven galaxies have been studied in this group; the average ages of the stellar populations in the nuclei and central spheroids vary in the range from 1.5–3 Gyr (in the E-galaxy NGC 83 and S0-galaxy IC 1548) to more than 10 Gyr, in NGC 79 (elliptical galaxy) and IC 1541 (lenticular galaxy). Finally, in the NGC 524 group, where the X-ray gas is located only in the compact halo around the central galaxy, all the group galaxies outside this halo demonstrate a synchronous evolution of the central regions [11].

In this paper we present the results of an analysis of the stellar population properties of the galaxies of another massive group with X-ray gas—the NGC 2300 group.

2. NGC 2300 GROUP: BASIC INFORMATION

The NGC 2300 group was identified a long time ago and has been studied ever since, because it is close to us and conveniently positioned in the northern sky. It appeared as far back as the catalog [12]—but only three galaxies were listed as its members at the time. Later, Garcia [13] compiled a list of thirteen members of NGC 2300 group, with the brightness of up to $B_0 = 14\overset{\mathrm{m}}{.}0$ (given the distance to the group of 30.3 Mpc, according to EDD [14], this gives a lower luminosity limit for the galaxies on Garcia's list of $M_B = -18\overset{\mathrm{m}}{.}4$); moreover, most of these thirteen group members—eleven galaxies—are spiral or irregular. In a recent revision of the list of groups in the nearby Universe [1], the NGC 2300 group is already divided into two parts—eleven galaxies belong to the group NGC 2300 itself, whereas two galaxies are assigned to the group NGC 2276—a galaxy second in brightness after NGC 2300, and of a rather late Sc-type at that. The division was done not according to the positions of the galaxies in the sky, but according to their radial velocity distribution, which does appear to be bimodal. It is interesting to note that the total list of thirteen, or $11 + 2$, galaxies differs by half (six objects) from the Garcia's list [13]; however, in terms of the morphological composition, both groups still contain mainly late-type galaxies. Only NGC 2300 itself, IC 455, and possibly, UGC 3654 are classified as lenticular galaxies in the NGC 2300/NGC 2276 group; there are no elliptical galaxies at all.

Such a late-type morphological composition is not very traditional for a massive group, considering the fact that the group also contains a rather noticeable hot intergalactic medium—the X-ray gas. The NGC 2300 group was the first, widely advertised example of a relatively poor group of galaxies, for which a reliable X-ray signal from the hot diffuse medium was discovered in the ROSAT data [18]. It is of interest that the centroid of the distribution of X-ray radiation, shown in [18], did not coincide with NGC 2300 — it was located in an empty spot between NGC 2300 and NGC 2276. Both galaxies have the same blue luminosity, but significantly different luminosities at 2 μm [1], i.e., NGC 2300 is a lot more massive than NGC 2276. Their systemic velocities differ by 500 km s^{-1}. Since the morphology of NGC 2276 in the optical range [19] and in the radio range [20] demonstrates a cometary shape, this galaxy is considered to move fast relative to the hot gas of the group, which strips one of sides of its disc by ram pressure. In this case, NGC 2300 should undoubtedly be considered the central galaxy of the group, although it is shifted relative to the centroid of the gas temperature distribution. Although the hot gas component of the NGC 2300 group is rather extended—the authors of [18] see it at least to a distance of 300 kpc from the group center—the group galaxies are distributed in an even greater area, and many of them lie outside the registered X-ray spot.

The list of the bright galaxies studied in this work and their characteristics from the literature are listed in Table 1.

The results of our recent photometric analysis of these five galaxies, based also on the data from

Table 1. Global parameters of the studied galaxies

Galaxy	NGC 2300	IC 455	IC 469	IC 499	UGC 3654
Morphological type (NED[1], LEDA[2])	SA 0^0	S0	SAB(rs)ab:	Sa	compact, S0
R_{25} (RC3[3], LEDA), arcsec	85	33	66	63	32
B_T^0 (RC3, LEDA)	11.77	14.01	12.87	12.91	14.61
M_B (RC3 + EDD[4])	−20.6	−18.4	−19.5	−19.5	−17.8
V_r (NED), km c^{-1}	1905	2050	2080	1882	2303
Distance from the group center (NED), kpc	0	95	383	716	144
Distance to the group[5], Mpc			30.3		
Photometric bulge parameters, from Ilyina and Silchenko [15]					
$r_{\rm eff}$, arcsec	5.8[6]	1.8	–	4.8	2.0
$n_{\rm Sersic}$	1.3[6]	2.5	–	2.2	2.6
Kinematic bulge parameters, based on this work					
$V_{\rm rot}(r_{\rm eff})$, km s^{-1}	14	36	–	67	27
$\sigma_*(r_{\rm eff})$, km s^{-1}	223	104	–	82	92

[1]NASA/IPAC Extragalactic Database

[2]Lyon–Meudon Extragalactic Database

[3]Third Reference Catalogue of Bright Galaxies [16]

[4]The Extragalactic Distance Database, `http://edd.ifa.hawaii.edu`

[5]Cosmicflow-1 [14]

[6]the metric parameters of the NGC 2300 bulge are given according to [17]

SCORPIO/BTA [15], are further used to separate the intervals of radii dominated by bulges and large-scale discs.

3. OBSERVATIONS AND DATA REDUCTION

We have obtained panoramic spectroscopic data for the central regions of five largest early-type disc galaxies of the NGC 2300 group using the Multi Pupil Fiber Spectrograph (MPFS) mounted at the primary focus of the 6-m telescope of SAO RAS [21]. The EEV42-40 CCD-array with 2048×2048 elements was used as a detector. During the MPFS observations, a set of square micro lenses, shaped into a square field of view with a size of 16×16 elements, constructed a pupil matrix, which was fed by means of fibers to the diffraction spectrometer slit. This configuration allowed us to simultaneously register 256 spectra, each of which characterized a spatial element of the galaxy image with a size of about $1''.0 \times 1''.0$. To study stellar populations and stellar kinematics, we observed the blue-green spectral range (4150–5650 Å) with an reciprocal dispersion of 0.75 Å pix^{-1} (spectral resolution of about 3 Å). For the emission line galaxy IC 469 we also obtained a spectrum in the red spectral range of 5800–7200 Å, in order to use the [NII]λ6583 line to study the kinematics of the gas component in the center of that galaxy. We calibrated the wavelength scale by taking a comparison spectrum of a helium-neon-argon lamp every time before and after the target spectrum; to correct for vignetting and different micro lens transmittance we used the internal lamp of the spectrograph and the twilight spectrum. The initial data reduction—bias subtraction, cosmic ray hits removal, extraction of one-dimensional image-element spectra from the CCD format, calibration of the selected spectra to the wavelength scale—was carried out in our original software package [21] in IDL environment.

Long-slit spectral observations were conducted with the multi-mode focal reducers SCORPIO [22] and SCORPIO-2 [23] at the 6-m telescope of SAO RAS. Overall, we obtained four slices for different position angles for NGC 2300 and several slices along the major axis for IC 455 and IC 499. The full log of exposures that we used for analysis is given in Table 2.

Table 2. Spectral observations of the NGC 2300 group with the BTA

Galaxy	Date	T_{exp}, min.	Range, Å	$FWHM_*$, arcsec	PA (top), deg
MPFS					
NGC 2300	Sep 24, 2001	60	4150–5650	1.9	174
IC 455	Sep 17, 2006	60	4150–5650	2.0	123
IC 469	Oct 02, 2005	45	6100–7100	1.5	88.5
IC 469	Oct 02, 2005	60	4150–5650	1.5	88.5
IC 499	Oct 18, 2006	60	4150–5650	1.5	178
UGC 3654	Aug 21, 2007	120	4150–5650	1.5	178.5
SCORPIO and SCORPIO-2					
NGC 2300	Feb 24, 2014	60	3700–7200	1.3	310
NGC 2300	Nov 20, 2014	60	3700–7200	1.7	21
NGC 2300	Mar 27, 2015	60	3700–7200	2.3	74
NGC 2300	Oct 09, 2015	120	4800–5500	4.5	170
IC 455	Dec 19, 2014	60	3700–7200	2.3	82
IC 499	Dec 19, 2014	60	3700–7200	2.3	78
IC 499	Mar 18, 2013	60	4800–5500	4.0	76

We used primarily a slit width of 1″, which facilitated a spectral resolution of 2.2 Å for observations with the VPHG2300G grism (SCORPIO) and about 5 Å—for observations with the VPHG1200@540 grism (SCORPIO-2). The sufficiently deep data that we obtained allowed us to study the stellar kinematics and stellar population properties in the discs up to the visual boundaries of the galaxies.

When computing the kinematic parameters of the stellar component—radial velocities and stellar velocity dispersions—we subtracted the continuum in every point of the galaxy. Then, after applying a logarithmic scale, it was subject to cross-correlation with spectra of G8–K2 giant stars with known radial velocities, observed on the same night and with the same equipment as the galaxy; we also sometimes used the dawn sky spectrum for cross-correlating (G2-type). The accuracy of the wavelength scale and the zero-point of the measured velocities were controlled by using the [OI]λ5577 Å night sky line. After obtaining the kinematic parameters, to analyze the stellar population properties—ages, general metallicities, and abundance ratios of magnesium (an alpha-element representative) and iron—we computed the Lick indices Hβ, Mg b, Fe 5270, and Fe 5335 for each individual spectrum. The definition of the Lick system of indices for absorption lines was taken from the works by Worthey et al. [24, 25]. The parameters computed from individual spectra obtained with the MPFS were then assembled into maps of central galactic regions. The derived maps of Lick indices—$\langle \mathrm{Fe} \rangle \equiv (\mathrm{Fe}\,5270 + \mathrm{Fe}\,5335)/2$, H$\beta$, and Mg b—are presented in Figs. 1–5. Various detailed model computations were done for these absorption lines within the framework of the evolutionary stellar population synthesis, linking the indices (equivalent width of absorption lines) with the average (stellar-luminosity weighted) stellar population properties—the so-called SSP-equivalent (SSP≡"Simple Stellar Population") ages and metallicities. Among the available models we chose the models of Thomas et al. [26], as they are computed for several magnesium-to-iron abundance ratios, and therefore, allow one to determine this third stellar population parameter in addition to the age and general metallicity.

4. RESULTS: STELLAR POPULATION

We used the Lick index maps for the central regions of the galaxies under study (Figs. 1–5) to estimate the average parameters of the stellar populations in the nuclei and bulges by comparing our measurements with the SSP-models of Thomas et al. [26]. The stellar nuclei of galaxies were identified as the

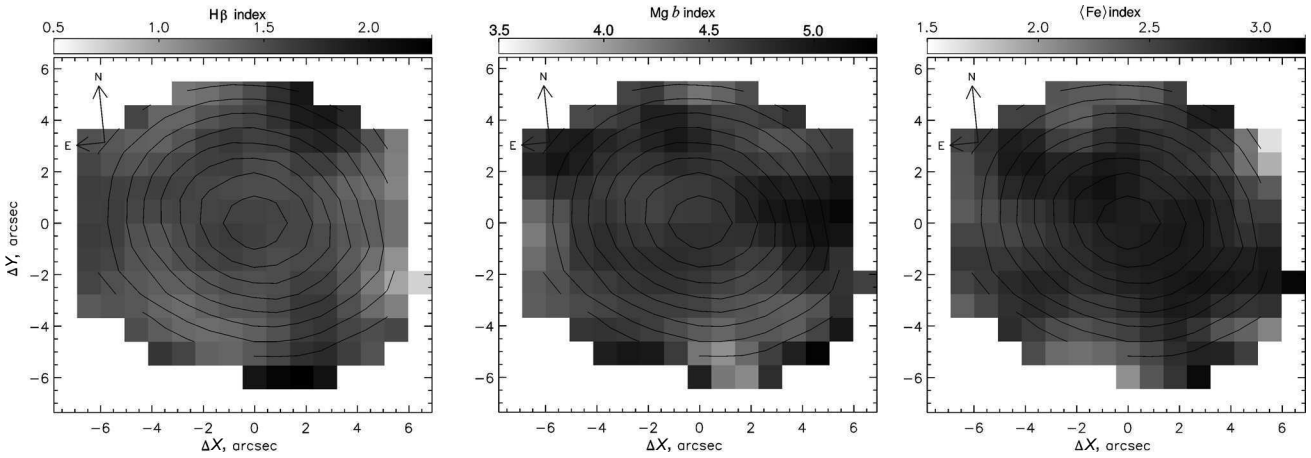

Fig. 1. Maps of the Lick indices Hβ, Mgb, $\langle \mathrm{Fe} \rangle \equiv (\mathrm{Fe}\,5270 + \mathrm{Fe}\,5335)/2$ for the central region of NGC 2300 based on the MPFS data. The isophotes show the surface brightness distribution in the continuum at the wavelength 5000 Å.

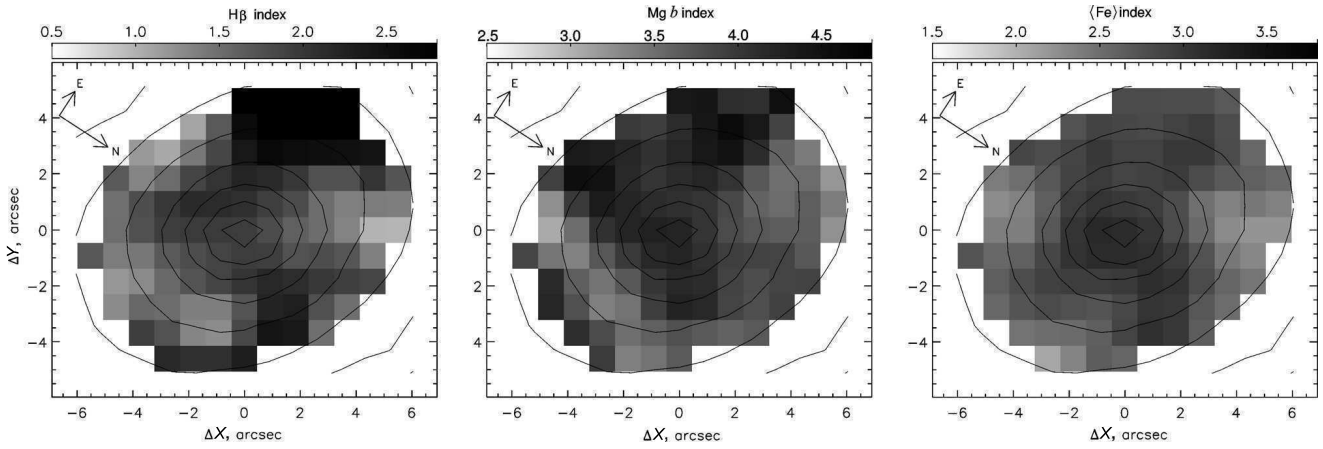

Fig. 2. Same as in Fig. 1, but for IC 455.

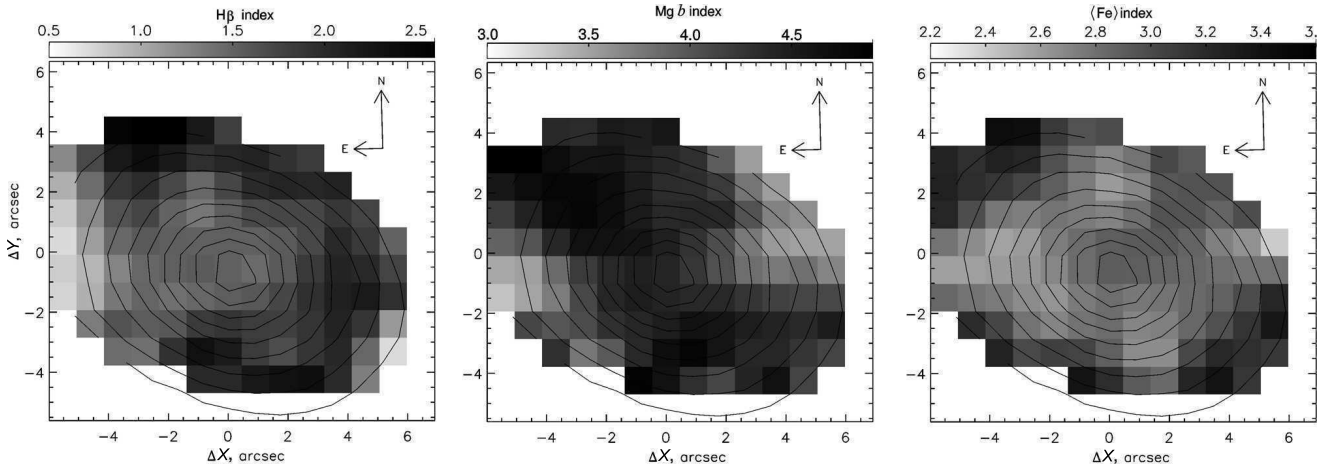

Fig. 3. Same as in Fig. 1, but for IC 499.

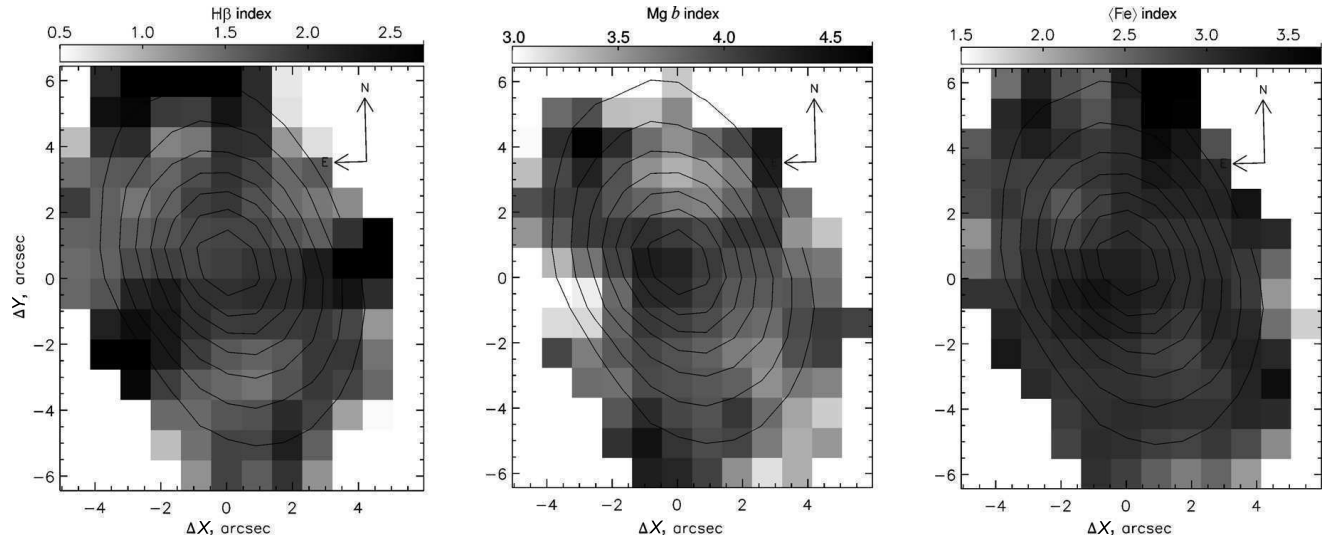

Fig. 4. Same as in Fig. 1, but for UGC 3654.

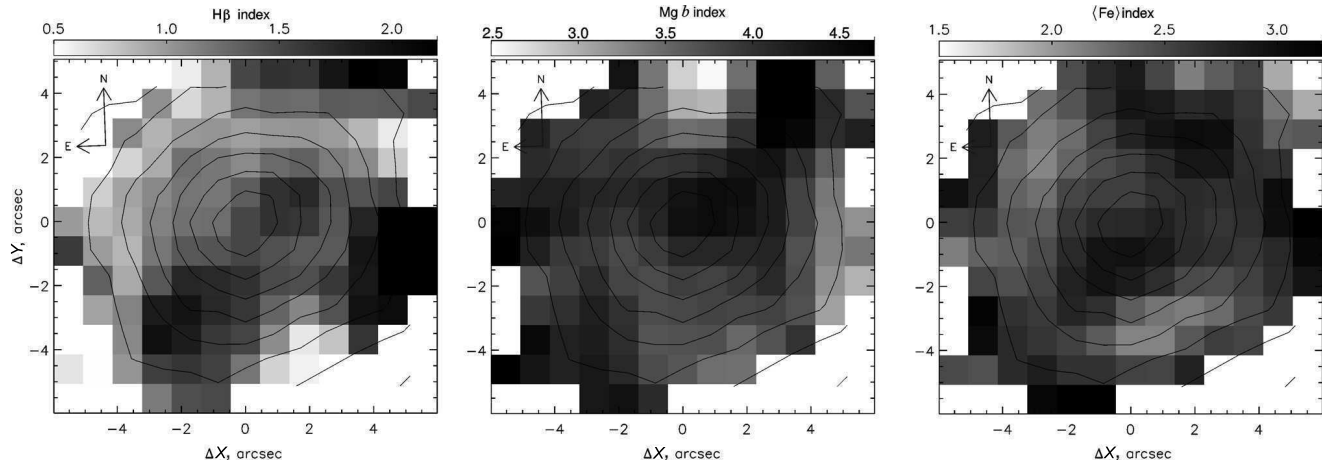

Fig. 5. Same as in Fig. 1, but for IC 469.

brightest spaxel (spatial element). To localize the bulges, we had to find a compromise between the effective radius of galactic bulges (Table 1) and the spatial resolution of our data (Table 2), which amounted to 1.″5–2″ for the MPFS observations. As a result, to avoid "contamination" by the bright nucleus in our bulge parameter measurements, we used the mean values of the indices in the ring zones with an inner radius of 3″. The outer radius of the ring zone was bounded by the MPFS field of view, but was taken to be no greater than 5.″5 for galaxies with compact bulges. The accuracy of the Lick indices for galaxy nuclei is about 0.1 Å, and for the bulges, thanks to the averaging over large amounts of spaxels, it is slightly higher—0.05–0.07 Å. This allows us to determine the metallicity of the stellar population with an inner accuracy of 0.05–0.1 dex, and the age—with an accuracy of 0.5 Gyr for $T < 5$ Gyr, 1 Gyr—for T from 5 to 9 Gyr, and with an accuracy of 3 Gyr for the old populations, $T \geq 10$ Gyr.

The stellar population parameters of the studied galaxies are presented in Tables 3 and 4—for the nuclei and bulges, respectively. Evidently, no synchronous evolution of the central regions is observed for this group of galaxies: the average age scatter for the stellar populations of both the nuclei and bulges ranges from 2 to 15 Gyr. In this regard, the NGC 2300 group turned out to be similar to other groups of galaxies, with a noticeable presence of a hot intergalactic medium. It resembles the group NGC 80 most of all, where the stellar population is

Table 3. Lick indices and parameters of the stellar population in the nuclei according to the MPFS data

Galaxy	Hβ	Mg b	⟨Fe⟩	T, billion years	[Z/H]	[Mg/Fe]
NGC 2300	1.64	5.19	2.87	7	+0.4	+0.35
UGC 3654	1.88	4.31	3.155	4	+0.5	+0.14
IC 455	2.23	4.34	3.25	2	+0.8	+0.13
IC 469	1.00	4.70	2.88	15	+0.2	+0.23
IC 499	1.60	4.46	2.97	10	+0.3	+0.17

Table 4. Lick indices and parameters of the stellar population in the bulges according to the MPFS data

Galaxy	Hβ	Mg b	⟨Fe⟩	T, billion years	[Z/H]	[Mg/Fe]
NGC 2300	1.52	4.83	2.87	11	+0.3	+0.26
UGC 3654	2.18	3.84	2.97	2	+0.55	+0.13
IC 455	1.90	3.93	2.68	6	+0.2	+0.19
IC 469	1.47	3.91	2.56	15	−0.1	+0.20
IC 499	1.87	4.19	2.76	5	+0.3	+0.21

also the oldest in the disc galaxies of the peripheral regions, and the central galaxy of the group contains an intermediate-age stellar component in the nucleus [10]. Such a similarity is probably related to a similar dynamical evolution of the groups: in the case of the NGC 80 group we observe a recent merger of the NGC 80 and NGC 83 [10] subgroups, whereas in the case considered in this work, we can suggest a currently developing process of falling of the NGC 2276 group into the main group of NGC 2300. Note that the youngest stellar population and the closest to solar abundance ratios of magnesium and iron in the bulge is observed in the lenticular galaxy UGC 3654, which belongs to the group NGC 2276 and which is probably currently moving together with NGC 2276 into the gravitational field and X-ray halo of the NGC 2300 group. The dynamical interaction of UGC 3654 with the NGC 2300 group is precisely what could have caused the recent star formation in its center, and quite possibly a structure transformation, including the evolution of the bulge and the steepening of its Sersic index [15].

For three galaxies of the group we also have deep spectral data, obtained with a long slit. This allows us to estimate the stellar population parameters in the outer large-scale discs of the galaxies. Figure 6 presents diagnostic diagrams, which we use to trace the variation of the average metallicity and age of the stellar population along the slit in IC 455, IC 499, and NGC 2300. All three outer discs turned out to be old, older than 8 Gyr, with lower-than-solar metallicities—as we expected to see in early-type disc galaxies in a massive group environment [28]. It is interesting to note that the inner stellar ring at a radius of 18″–30″ in the IC 499 galaxy has also turned out to be old, $T = 10 \pm 2$ Gyr.

5. RESULTS: STELLAR KINEMATICS AND GAS COMPONENT

Panoramic spectroscopy with MPFS, which allows us to build two-dimensional radial-velocity fields for the stellar component of the central regions, makes it possible to derive conclusions about the nature of the rotation and about the dynamic status of the bulges of the galaxies under investigation. Table 1 gives the averaged line-of-sight projections of the rotation velocities and the stellar velocity dispersions at the effective radius for four galaxies in the sample—except IC 469, for which we found no bulge at all in our photometric analysis [15]. The Binney–Kormendy diagram, which links the ratio of the stellar-component ordered rotational velocity to the line-of-sight projection of the stellar velocity dispersion (i.e., with account for the inclination of the rotation axis to the line of sight) and the visible isophote ellipticity, allows one to estimate the dynamic status of the stellar system. When we see the sky-projection of the spheroidal body of a galaxy, the isophote ellipticity presents a combination of internal flattening of the spheroid and an inclination of its symmetry axis to the line of sight. Comparing on this diagram our measurements with the dynamical models of spheroids of different shapes, we can make a conclusion about whether a galaxy is an axisymmetric body rotating about its shortest (oblate) axis, or about its longest (prolate) axis, or it is a triaxial spheroid, the shape of which is sustained by the anisotropic distribution of chaotic stellar motions (stellar velocity dispersion). Figure 7 shows the Binney–Kormendy diagrams marked with the kinematic data from Table 1 compared to the isophote ellipticity based on our photometric data [15]. As is evident from the diagram to the left, the bulges of three galaxies, IC 499, IC 455, and UGC 3654, do not differ from the typical bulges of lenticular galaxies (reference sample—lenticular field galaxies from [29]), and from the diagram to the right—that they may well be described as oblate

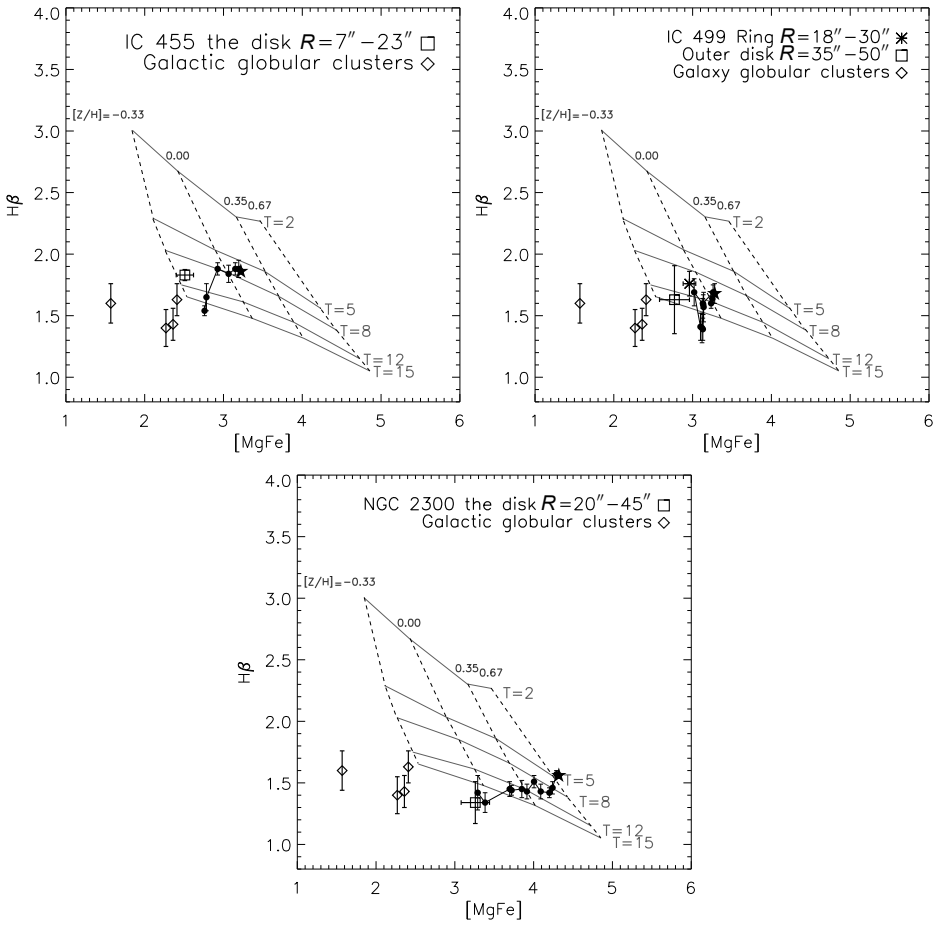

Fig. 6. "Index–index" diagnostic diagrams for measuring the ages and metallicities of the stellar populations along the radii of three galaxies belonging to the NGC 2300 group, based on the long-slit spectroscopy data (black dots with error bars). Individual symbols show: the five-pointed filled star—the indices for galaxy nuclei, squares—indices for the outer stellar discs of the galaxies, and the eight-pointed "star" symbol—the stellar ring in IC 499. The solid lines are the equal-age stellar population models [26]; the ages of the models are given in Gyr; the general metallicity of the models is shown near the model reference marks, connected by dashed lines. For comparison, the diamonds show several globular clusters of the Galactic bulge with ages of about 10 Gyr and metallicities of [Z/H]= $-0.4 \ldots -0.7$ dex taken from [27].

spheroids, the flattening of which corresponds to their ratio of the rotation velocity to the stellar velocity dispersion. Note that the domination of rotation in the stellar-component kinematics in IC 499 is more evident than in model oblate spheroids. It can be suggested that the bulge of IC 499 can be classified more accurately as a pseudo-bulge—a bulge that had formed from the disc matter over the course of the secular evolution of the galaxy. This is also not contradicted to the lower, compared to the other galaxies, Sersic index, which characterizes the profile shape of the surface brightness of the bulge (Table 1). Conversely, the main galaxy of the NGC 2300 group differs sharply in its central dynamics both from the other galaxies in the group, and from lenticular galaxies as a class: it demonstrates an anomalous low rotation velocity at the effective bulge radius and falls into the triaxial spheroid category—together with a whole class of giant elliptical galaxies. As we shall see below, the "disc" of NGC 2300 also demonstrates kinematics completely non-typical for disc galaxies as a class.

In Fig. 8 we compare the orientations of the kinematic (based on the MPFS observational data) and photometric (from [15]) major axes of the central stellar component in all galaxies with noticeable central rotation. The kinematic major axis is the direction of maximal stellar line-of-sight velocity gradient on a two-dimensional velocity distribution, and the photometric major axis is the major axis of isophotes. In the case of circular rotation and axisymmetric density distribution, both directions coincide with the line of nodes of the rotation plane; i.e., in the case of circular rotation, we should observe a coincidence of the kinematic and photometric major axes. If the mass distribution is not axisymmetric and the rotation is non-

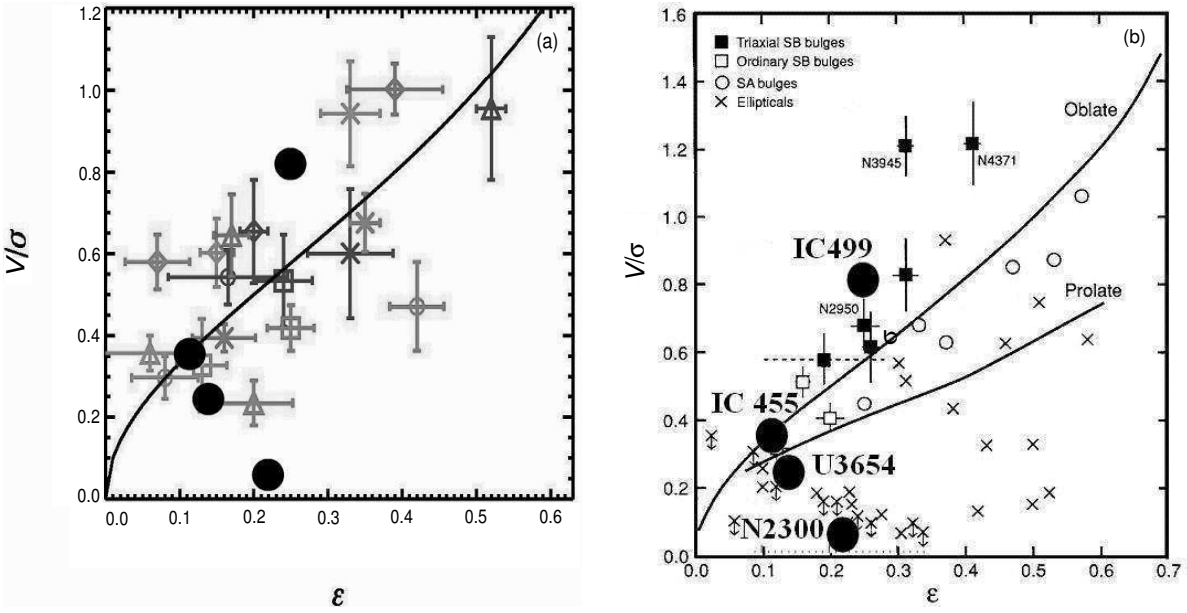

Fig. 7. The Binney–Kormendy diagrams for estimating the dynamic temperature of the bulges of the NGC 2300 group galaxies (large black circles). Left figure—a comparison of the bulges of NGC 2300 group galaxies with the bulges of isolated S0-galaxies, an adaptation of Fig. 5 from [29]; all galaxies except NGC 2300 demonstrate normal flattened spheroids, whose shape is sustained by rotation. Right figure—a comparison of the bulges of NGC 2300 group galaxies with different types of spheroids, an adaptation of Fig. 17 from [2]; evidently, NGC 2300 belongs to a class of non-rotating spheroids with an anisotropic stellar velocity dispersion, and IC 499—to a class of pseudo-bulges, which are often encountered in disc galaxies with bars.

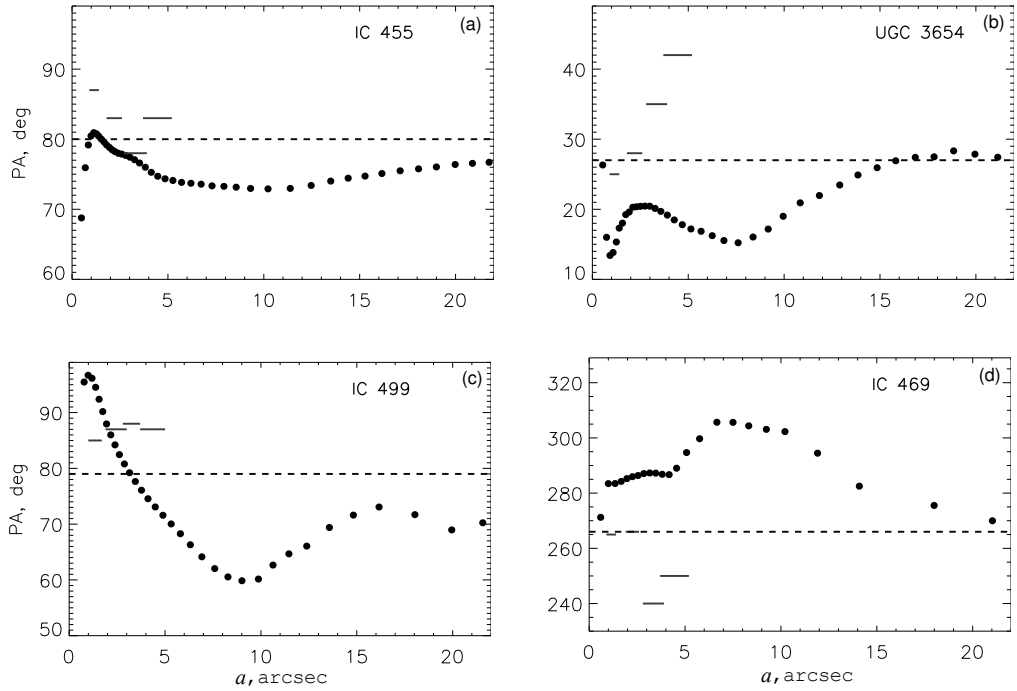

Fig. 8. A comparison of the orientation of the isophote major axis (black dots) with the kinematic major axis of the stellar component (horizontal dashed line). The dashed line shows the orientation of the line of nodes of the outer stellar disc.

circular because of that, the kinematic and photometric major axes will not coincide with the line of nodes of the rotation plane; moreover, in an image plane projection, they will deviate from the line of nodes in opposite directions (see, e.g, the models in [30]). In Fig. 8, this behavior of the kinematic and photometric major axes can be seen in the case of UGC 3654 and IC 469; this is a typical manifestation of the presence of a bar. The bar is also present in IC 455, however, it is rather compact and sunk in the bulge, therefore the deviation of the kinematic major axis from the line of nodes is weak. As for the photometry, the bar is visible only in the residual surface brightness maps, after subtracting the bulge model, and also in the color map [15]. The case of IC 499 is of special interest. A large turn of isophotes is observed in the center of the galaxy; however, the kinematic major axis of the stellar component turns *together* with the isophote major axis. In this galaxy, one can suspect the presence of not a bar, but a inclined circumnuclear stellar disk, or a bulge whose rotation axis is inclined relative to the rotation axis of the outer disc.

The spectra obtained in the long-slit mode were used to study the large-scale kinematics of the stellar discs of the group galaxies.

IC 455. Emission lines are absent in the spectrum of the galaxy up to the visual boundaries of the disc. Thus, there is no ionized gas in this lenticular galaxy. The stellar component rotates regularly; additionally, the rotation curve is not flat, as is usual for disc galaxies, but with a drop in the rotation velocity near the boundaries of the stellar disc (Fig. 9, left). Considering the fact that the exponential scalelength of the stellar disc of IC 455 is equal to $7''.6$ [15], and the maximum of the rotation curve is reached at $R \approx 15''$, i.e., approximately at the radius of double exponential radial scale, we can conclude that the rotation of the galaxy within its optical radius is determined by the stellar disc, and dark matter does not exert in the dynamics.

NGC 2300. This galaxy, classified photometrically as disc-type, does not rotate at all according to our data. In Fig. 7 we saw that its bulge, despite the rather elongated isophote shape, shows quite a low visual rotation velocity with regard to the stellar velocity dispersion. As is evident in Fig. 10, the rotation velocity drops to zero beyond the region where the bulge dominates. We have obtained four spectra of the galaxy with different orientations of the long slit; the position angles of the cross-sections were varied with steps of 30°–55°. None of the slit orientations have shown rotation for the outer regions of NGC 2300. The stellar velocity dispersion remains high, about 150 $\mathrm{km\,s^{-1}}$, up to the optical limits of the galaxy (Fig. 11, right). From the kinematic characteristics, we conclude that NGC 2300 is not a disc galaxy, but an elliptical galaxy, probably of triaxial shape. We have reached the same conclusion earlier based on the photometric analysis of the surface brightness distribution of NGC 2300 [15].

IC 499. This galaxy has ionized gas, and the strengthening of emission lines at the distances of $20''$–$30''$ and about $55''$ from the center indicates a presence of a series of rings. The rotation curve of the stellar component is flat up to the optical boundaries of the disc (Fig. 9, right); the gas and stars rotate in a similar fashion, the slight lag of the stars can be explained by an asymmetric drift. Figure 11 (left) shows the line-of-sight projection of the velocity dispersion profile of the stellar component based on the spectral data with a resolution of about 2 Å (see Table 2). Evidently, starting from the radius about $20''$, a relatively cool stellar component dominates in the dynamics—a disc, with a velocity dispersion of 40–70 $\mathrm{km\,s^{-1}}$. Some asymmetry is possible in the velocity dispersion distribution of the disc stars: the East side of the disc is cooler dynamically than the West side. This fact is in full agreement with the characteristics of the current star formation precisely to the East of the center (see below).

The ionized gas in the extended disc of IC 499, noticeable by the emission lines in the spectrum, can be excited in different ways—by young massive stars, i.e., by the ongoing star formation, or by shock waves, which may arise in the case of non-circular gas motions, i.e., when the distribution of mass in the galaxy is not axisymmetric, or when an external object falls into the galaxy disc. A method exists of comparing the flux ratios of high- and low-excitation emission lines to diagnose the source of gas excitation—the so-called BPT-diagrams [31–33]. Figure 12 shows the BPT-diagrams for the emission spectrum of IC 499 at different radii, compared with the models [34] and the data for several thousand nuclei of nearby galaxies from the SDSS survey. The positive radius values are related to the eastern part of the slit, the negative ones—to the western part. The regions where the gas is excited by young massive stars fall to the left of the dashed line, and the ones where gas is excited by shock waves are located to its right; the middle position is characterized by emission-line spectra of gas with an intermediate excitation type. A strong West-to-East asymmetry can be noticed in the disc of IC 499: to the East from the nucleus, the rings of ionized gas can be excited—at least, in part—by young stars, and to the West of the nucleus—only by shock waves. It is interesting to note that the same asymmetry is noticeable also in the color map of IC 499 [15]: to the East of the nucleus, at the distances of about $25''$ and $50''$ from the center, blue arcs can be seen on the major axis, and especially blue is the appearance of the outer arc, imbedded in the

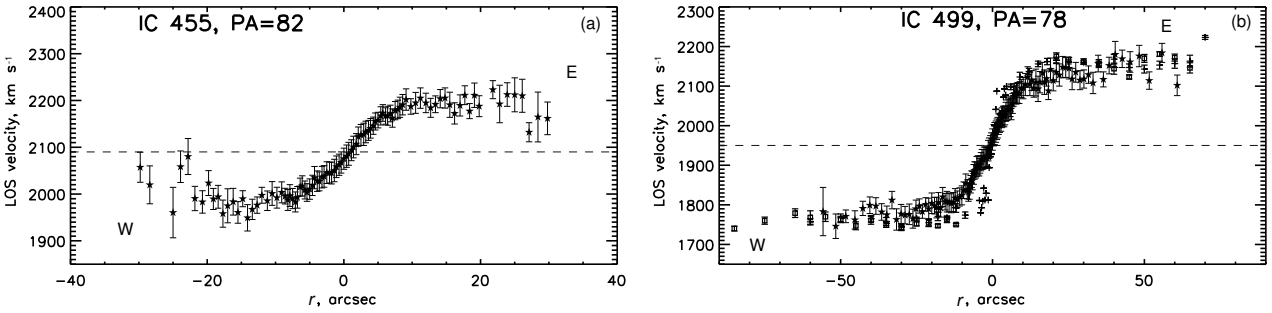

Fig. 9. Stellar line-of-sight velocity profiles along the major axis for IC 455 and IC 499 (stars). The velocities of ionized gas measured from the emission lines [NII] λ 6583 (pluses) and Hα (squares) are also shown for IC 499.

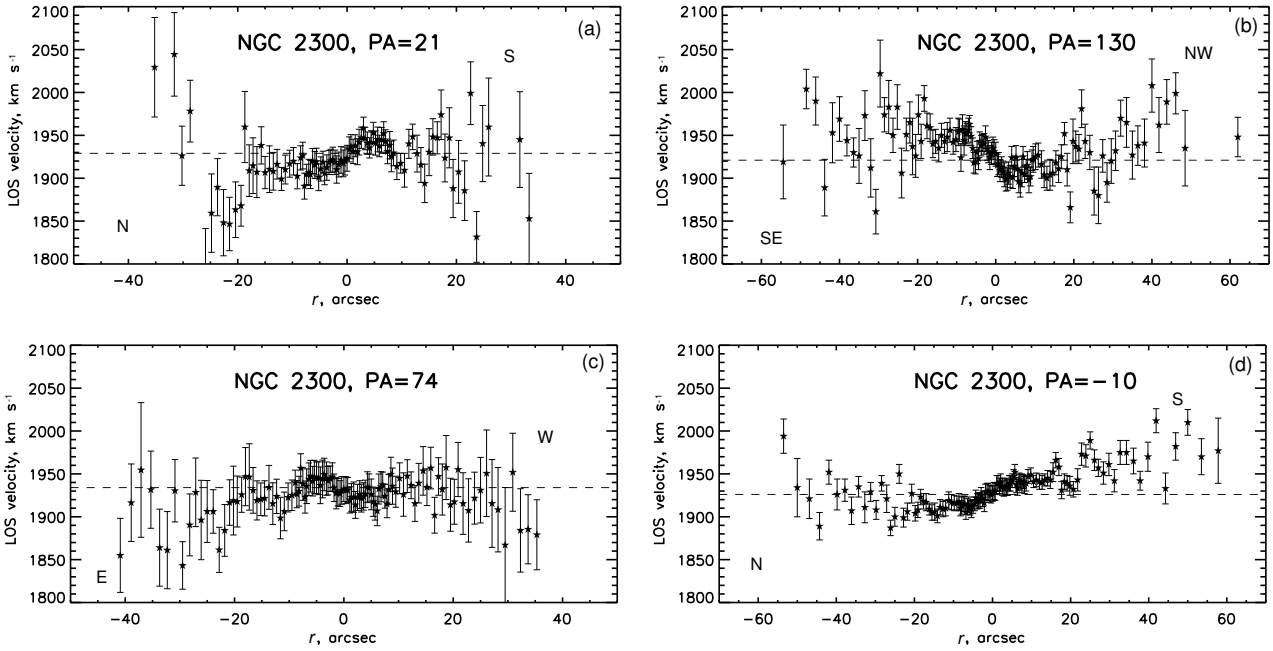

Fig. 10. Kinematic slices — stellar line-of-sight velocity profiles of NGC 2300 for different position angles.

blue ring of the young stellar population, whereas the stellar disc to the West of the center appears homogeneously red. Overall, at close scrutiny, IC 499 appears to be not a spiral (Table 1), but a lenticular galaxy with a system of star-forming rings. Moreover, the asymmetry in the color distribution and the emission line ratio observed *along* the major axis indicates a wave-like distortion of the gaseous disc with respect to the stellar one. This conclusion is also in agreement with the tilted rotation of stars in the galactic center. The gas with the tilted momentum was most likely accreted from outside, but quite a long time ago, and it had time to settle into the main plane of symmetry of the galaxy, retaining only a residual precession.

6. CONCLUSION AND DISCUSSION

The paper presents the results of the spectral investigation of the stellar populations and kinematics of five galaxies of the NGC 2300 group. The group is rather large, about 10^{13} Solar masses according to [1], and contains hot intergalactic medium [18]. As a result of our study, we have determined that, as in the case of other groups with X-ray gas, the galaxies of the NGC 2300 group do not demonstrate a synchronous evolution of their central regions: the average age of the stellar populations of the nuclei and bulges in the galaxies ranges from 2 to 15 Gyr. This can be understood within the framework of the hierarchical model of "gathering" of massive agglomerates of galaxies: if two groups, each of which already has a hot X-ray halo, merge (as we noted

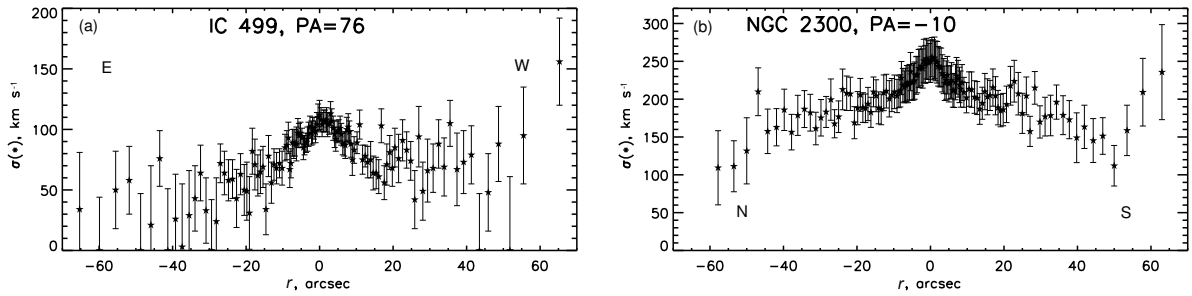

Fig. 11. Stellar velocity dispersion profiles for IC 499 and NGC 2300.

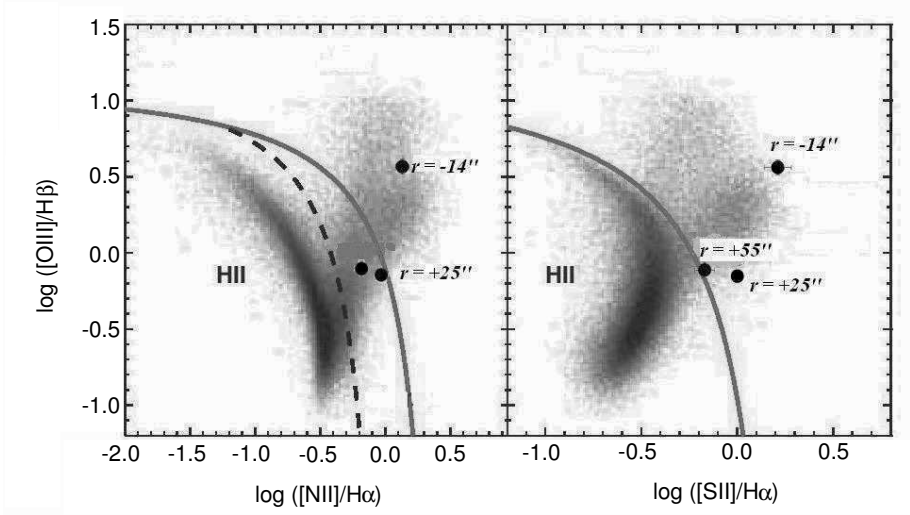

Fig. 12. Diagnostic diagrams for determining the excitation mechanism of the ionized gas in the disc of IC 499. The curves divide the regions of excitation by young stars (left) and shock waves (right) — an adapted scheme of Fig. 1 from [34]. The grey cloud of dots shows several thousand galaxy nuclei from the SDSS. The dots marked by radius values are our measurements of emission line ratios of IC 499 at the given distances from the center.

in the case of the group NGC 2300/2276 and earlier in the case of group NGC 80/83 [10]), then the group member galaxies, embedded in hot intergalactic medium, should no longer have external reservoirs of cool gas. If an X-ray halo is absent, then every disc galaxy should have such a reservoir, and as they approach one another during the formation of a group, gravitational tides stimulate the inflow of cold gas from the outer reservoirs into the inner regions of the galaxies, with consequent bursts of star formations and the "rejuvenation" of the central regions, which we observe as synchronous evolution, e.g., in the NGC 524 [11], NGC 3169 [5], NGC 5576 [4], and NGC 3379 [3] groups. A separate question—regarding the presence of an X-ray halo in half the groups of galaxies and its absence in the other half, despite similar dynamic masses [35]—has not yet been answered.

A detailed investigation of the central galaxy of the NGC 2300 group has confirmed our suspicions [15]—that despite the sparse extended star halo and the SA0 classification in all recent catalogs, the galaxy is not disc-type. A kinematic analysis of the stars in the center of NGC 2300 alone allows us to classify it as a so-called "slow rotator"—a triaxial stellar spheroid, the elongated shape of which is sustained by the anisotropic distribution of the stellar velocity dispersion. Our deep long-slit spectra, which allowed us to study the stellar kinematics also in the region of the assumed stellar-disc dominance (isolated by the exponential profile of the surface brightness in [15]), have shown that there is even less ordered stellar-component rotation in the outer regions than in the inner ones. Furthermore, within the accuracy limits of our measurements, we have not detected any rotation at all, and this means that the outer regions of NGC 2300 do not constitute a disc. Probably, NGC 2300 is a smaller analog of the central galaxies in clusters, the cD-galaxies, which also demonstrate less steep (compared to the Vaucouleurs law) surface brightness profiles in the outer regions [36]. Being located in the center of a potential well of massive

dark halos, cD-galaxies absorb many other galaxies in their lifetimes, which happen to be too close to the center in the process of "gathering" into clusters or groups. Such products of multiple small mergers are dynamically hot [37].

ACKNOWLEDGMENTS

Observations with the 6-m BTA telescope are conducted with the financial support of the Ministry of Education and Science of the Russian Federation (agreement No14.619.21.0004, project identifier RFMEFI61914X0004). We thank for their support of our BTA observations the following staff members of SAO RAS: A.V. Moiseev, A.N. Burenkov, R.I. Uklein, A.A. Smirnova, D.I. Makarov. This research has made use of the Lyon–Meudon Extragalactic Database (LEDA), facilitated by the LEDA team on the Lyon observatory CRAL (France), and the NASA/IPAC Extragalactic Database (NED), operated by the Jet Propulsion Laboratory, California Institute of Technology, under contract with the National Aeronautics and Space Administration (USA). Spectral analysis of the NGC 2300 group galaxies was supported by the Russian Science Foundation grant 14-22-00041.

REFERENCES

1. D. Makarov and I. Karachentsev, Monthly Notices Royal Astron. Soc. **412**, 2498 (2011).
2. J. Kormendy and R. C. Kennicutt, Jr., Annual Rev. Astron. Astrophys. **42**, 603 (2004).
3. O. K. Sil'chenko, A. V. Moiseev, V. L. Afanasiev, et al., Astrophys. J. **591**, 185 (2003).
4. O. K. Sil'chenko, V. L. Afanasiev, V. H. Chavushyan, and J. R. Valdes, Astrophys. J. **577**, 668 (2002).
5. O. K. Sil'chenko and V. L. Afanasiev, Astronomy Letters **32**, 534 (2006).
6. S. Schneider, Astrophys. J. **288**, L33 (1985).
7. V. L. Afanasiev and O. K. Sil'chenko, Astron. and Astrophys. **429**, 825 (2005).
8. V. L. Afanasiev and O. K. Sil'chenko, Astron. Astrophys. Trans. **26**, 311 (2007).
9. O. K. Sil'chenko, A. V. Moiseev, and A. P. Shulga, Astron. J. **140**, 1462 (2010).
10. O. K. Silchenko and V. L. Afanasiev, Astronomy Reports **52**, 875 (2008).
11. O. K. Sil'chenko and V. L. Afanasiev, Astrophysical Bulletin **67**, 253 (2012).
12. J. P. Huchra and M. J. Geller, Astrophys. J. **257**, 423 (1982).
13. A. M. Garcia, Astron. and Astrophys. Suppl. **100**, 47 (1993).
14. R. B. Tully, L. Rizzi, E. J. Shaya, et al., Astron. J. **138**, 323 (2009).
15. M. A. Il'ina and O. K. Sil'chenko, Astronomy Reports **60**, 894 (2016).
16. G. de Vaucouleurs, A. de Vaucouleurs, H.G. Corwin, Jr., et al., *Third Reference Catalogue of Bright Galaxies*, Vol. 1: *Explanations and References* (Springer, New York, 1991).
17. E. Laurikainen, H. Salo, R. Buta, et al., Monthly Notices Royal Astron. Soc. **405**, 1089 (2010).
18. J. S. Mulchaey, D. S. Davis, R. F. Mushotzky, and D. Burstein, Astrophys. J. **404**, L9 (1993).
19. H. C. Arp, Astrophys. J. Suppl. **14**, 1 (1966).
20. J. J. Condon, Astrophys. J. Suppl. **54**, 459 (1983).
21. V. L. Afanasiev, S. N. Dodonov, and A. V. Moiseev, in *Proc. Conf. on Stellar Dynamics: from Classic to Modern, St. Petersburg, Russia, 2001*, Ed. by L. P. Osipkov and I. I. Nikiforov, (Saint Petersburg Univ. Press, 2001), p.103.
22. V. L. Afanasiev and A. V. Moiseev, Astronomy Letters **31**, 194 (2005).
23. V. L. Afanasiev and A. V. Moiseev, Baltic Astronomy **20**, 363 (2011).
24. G. Worthey, S. M. Faber, J. J. Gonzàlez, and D. Burstein, Astrophys. J. Suppl. **94**, 687 (1994).
25. L. A. Jones and G. Worthey, Astrophys. J. **446**, L31 (1995).
26. D. Thomas, C. Maraston, and R. Bender, Monthly Notices Royal Astron. Soc. **339**, 897 (2003).
27. M. A. Beasley, J. P. Brodie, J. Strader, et al., Astron. J. **128**, 1623 (2004).
28. O. K. Sil'chenko, I. S. Proshina, A. P. Shulga, and S. E. Koposov, Monthly Notices Royal Astron. Soc. **427**, 790 (2012).
29. I. Yu. Katkov, A. Yu. Kniazev, and O. K. Sil'chenko, Astron. J. **150**, id. 24 (2015).
30. A. V. Moisseev and V. V. Mustsevoi, Astronomy Letters **26**, 565 (2000).
31. J. A. Baldwin, M. M. Phillips, and R. Terlevich, Publ. Astron. Soc. Pacific **93**, 5 (1981).
32. S. Veilleux and D. E. Osterbrock, Astrophys. J. Suppl. **63**, 295 (1987).
33. D. E. Osterbrock, *Astrophysics of Gaseous Nebulae and Active Galactic Nuclei* (Univ. Science Books, Mill Valley, 1989).
34. L. J. Kewley, B. Groves, G. Kauffmann, and T. Heckman, Monthly Notices Royal Astron. Soc. **372**, 961 (2006).
35. J. S. Mulchaey, D. S. Davis, R. F. Mushotzky, and D. Burstein, Astrophys. J. Suppl. **145**, 39 (2003).
36. A. Oemler, Jr., Astrophys. J. **209**, 693 (1976).
37. A. Garijo, E. Athanassoula, and C. Garcia-Gomez, Astron. and Astrophys. **327**, 930 (1997).

Translated by E. Chmyreva